Real-time airport surface movement planning
Minimizing aircraft emissions

Evertse, C.; Visser, H. G.

DOI
10.1016/j.trc.2017.03.018

Publication date
2017

Document Version
Final published version

Published in
Transportation Research. Part C: Emerging Technologies

Transportation Research Part C 79 (2017) 224–241

Contents lists available at ScienceDirect

Transportation Research Part C

journal homepage: www.elsevier.com/locate/trc

Real-time airport surface movement planning: Minimizing aircraft emissions ☆

C. Evertse, H.G. Visser *

Faculty of Aerospace Engineering, Delft University of Technology, Delft, The Netherlands

ARTICLE INFO

Article history:
Received 11 August 2016
Received in revised form 13 March 2017
Accepted 26 March 2017
Available online 31 March 2017

Keywords:
Airport surface movement planning
Emissions
Mixed-integer linear programming

ABSTRACT

This paper presents a study towards the development of a real-time taxi movement planning system that seeks to optimize the timed taxiing routes of all aircraft on an airport surface, by minimizing the emissions that result from taxiing aircraft operations. To resolve this online planning problem, one of the most commonly employed operations research methods for large-scale problems has been successfully used, viz., mixed-integer linear programming (MILP). The MILP formulation implemented herein permits the planning system to update the total taxi planning every 15 s, allowing to respond to unforeseen disturbances in the traffic flow. Extensive numerical experiments involving a realistic (hub) airport environment bear out that an estimated environmental benefit of 1–3 percent per emission product can be obtained. This research effort clearly demonstrates that a surface movement planning system capable of minimizing the emissions in conjunction with the total taxiing time can be beneficial for airports that face dense surface traffic and stringent environmental requirements.

1. Introduction

Major hub airports are often confronted with the need to increase airside capacity, while meeting sustainability goals at the same time. Indeed, the increasing air traffic demand necessitates airports to find ways to increase their throughput capacity. Yet, at the same time airports also have to find a way towards more sustainable operations, as a result of more stringent environmental regulation and the growing awareness of sustainable development among the general public (Atkin et al., 2010; Visser et al., 2009).

During peak hours, major Air Traffic management (ATM) bottlenecks often occur in the terminal air space as well as on the airport ground surface, which can e.g. be observed by aircraft lining up in queues in front of runways or aircraft flying holding patterns in the terminal airspace. This problem of insufficient ATM capacity, not only results in a loss in efficiency, but it also leads to more environmentally demanding operations. Congestion problems can be resolved not only by increasing the throughput capacity of runway and taxiway systems, but also by making better use of the resources already available through improved airport terminal area operations. With respect to the latter issue, the current practice in routing and scheduling of airport surface traffic leaves ample room for improvement in terms of taxiway grid efficiency, notably through the introduction of advanced surface traffic automation systems Atkin et al. (2010).

☆ This article belongs to the Virtual Special Issue on "Technologies and Control for Sustainable Transportation".

* Corresponding author at: Faculty of Aerospace Engineering, TU Delft, P.O. Box 5058, 2600 GB Delft, The Netherlands.
E-mail address: h.g.visser@tudelft.nl (H.G. Visser).

http://dx.doi.org/10.1016/j.trc.2017.03.018
0968-090X/

This study focuses on the synthesis of optimal airport surface movement planning, anticipating the implementation of improved surface movement surveillance systems and avionics that enable pilots to follow a precisely timed taxiing route. Optimal taxi movement planning has the potential to reduce gaseous emissions and fuel burn of taxiing aircraft on airports, thereby helping airports to meet the imposed environmental regulations. To the best of the authors' knowledge, the problem of routing aircraft ground movements with the aim to optimize local emissions has yet to be adequately addressed. The development of a real-time surface movement planning system that allows to include (local) emission considerations in the optimal routing of the surface movements is the focus in this research.

This article is organized as follows. Firstly, the state of the art will be described in Section 2. Then, the requirements and preliminary design of the optimization-based planning system will be given in Section 3. This is then followed by a description of the employed fuel burn and emission models in Section 4. The technical implementation of the proposed planning system will be explained in Section 5. Finally, the results pertaining to a comprehensive case study and the conclusions will be given in Sections 6 and 7, respectively.

2. State of the art

This section presents a concise literature survey on existing research efforts related to the mathematical models and solution methods used in airport surface movement problems. A brief survey will be given particularly focusing on categorization according to the issues (1) solution methods, (2) optimization objectives, and (3) rolling time horizons.

A vast amount of research has been conducted in the last decade on the subject of surface movement planning optimization for taxiing aircraft on airports. The survey by Atkin et al. (2010) provides an excellent overview on ground movement planning formulations and resolution methods. This section repeats some of the main insights provided in Atkin et al. (2010), augmented with some more recent developments.

2.1. Solution methods

One of the most distinctive features in the reported studies on this subject relates to the type of solution method that has been used. Essentially, the following three different types of quantitative solution methods were found:

- *Mixed integer linear programming* (*MILP*). MILP is an exact method in the sense that it yields an optimal solution. Optimality is guaranteed unconditionally. Although the airport surface movement optimization problem is essentially NP-hard Clare and Richards (2011), the reported computational times are typically low, provided that the employed MILP problem formulation is not overly complex. It is noted that a mixed integer linear program considers a set of linear objectives and constraints, while some of the variables are defined as integers or binaries, leaving the rest as continuous variables. Successful examples of the use of MILP can be found in (Clare and Richards, 2011; Visser and Roling, 2003; Smeltink et al., 2004; Balakrishnan and Jung, 2007; Marín and Codina, 2008.).
- *Heuristics.* These are custom made algorithms, that are capable of finding a near-optimal solution within a relatively short time span. Although in theory heuristic algorithms offer a chance to find a global optimal solution, in practice that chance can be remote, as heuristics often get stuck at some local optimal solution. For some problems that are too hard to solve with an exact method, a heuristic might be used to explore the states of the problem that are most likely to contain the optimal solution. Examples of applications to the taxi movement planning problems are reported in (Ravizza et al., 2012; Weiszer et al., 2014).
- *Metaheuristics.* Metaheuristics can be used when exact optimization methods fail to generate a solution in an acceptable amount of computation time, or if they fail to generate a solution at all. Metaheuristic methods are capable of solving nonlinear problems and they can work with a higher problem complexity than MILP. Moreover, they are able to quickly generate multi-objective graphs or Pareto-fronts. A common characteristic of metaheuristics is that, in contrast to heuristics, they apply some kind of mechanism to avoid local optima or to provide the ability to move out of a local optimum. However, global optimality is still not guaranteed. Another disadvantage is that metaheuristics only outperform MILP in terms of computational speed in problems above a certain degree of complexity. See (Chen and Stewart, 2011; Chen et al., 2016; Pesic et al., 2001; Herrero et al., 2005; Garcia et al., 2005; Gotteland et al., 2003) for metaheuristics applied to the airport surface planning problem.

2.2. Optimization objectives

Airport surface movement optimization models can also be classified with respect to the main objectives considered. Objectives typically found in the literature include, total taxi time (Visser and Roling, 2003; Smeltink et al., 2004; Herrero et al., 2005; Ravizza et al., 2012) waiting times during the trajectory (Visser and Roling, 2003; Ravizza et al., 2012), fuel burn and emissions (Ravizza et al., 2012; Chen et al., 2015), delay (Visser and Roling, 2003; Herrero et al., 2005), taxi distance (Clare and Richards, 2011) and Central Flow Management Unit (CFMU) departure slot violation (Gotteland et al., 2003), or a combination of criteria (Chen et al., 2016). In Section 3 it will be outlined in detail which factors have been included in the objective function considered in this study.

2.3. Rolling time horizons

Using a rolling time horizon approach, the daily flight schedule can be split up into smaller sequential time frames, each covering only a portion of all the flights to be optimized. By breaking up a single large optimization problem into a sequence of smaller problems the response time needed for calculating a planning update is vastly improved. Moreover, the implementation of a rolling time horizon approach provides the opportunity to introduce feedback in the planning system, allowing to compensate for uncertainties in the flight operations (Clare and Richards, 2011).

In Smeltink et al. (2004) the three most commonly employed approaches to rolling time horizons are described:

- Hard-coded time horizon with fixed trajectory history. The size of the time horizon is pre-set, for example 15 or 30 min. Only aircraft that are ready for pushback or that touch down on the runway within the time horizon, are routed and scheduled. Aircraft that have been already routed in a previous time window will not change their taxi schedule. As a consequence, employing a short time horizon might result in many fixed trajectories, thus compromising the freedom to optimize. On the other hand, a long time horizon ensures near-optimal performance, but might increase the computational demand to an unacceptably large level.
- Hard coded time horizon with re-routings of previously routed aircraft. Again, the size of the time horizon is fixed, but aircraft that did not complete their trajectory within the time horizon can be rerouted or rescheduled for the rest of their trajectory. In some approaches, e.g. (Smeltink et al., 2004), aircraft trajectories that began within the time horizon, but expand beyond the end of the time horizon, are allowed to be completed. Other methods, e.g. (Clare and Richards, 2011), cut the aircraft trajectories where the time horizon ends, and use an approximation for the remainder of those trajectories.
- Sliding time window'. This type of time window is not pre-set, rather each new window starts exactly at the time when the next aircraft to be routed is ready for pushback or taxi-out. The size of the time window is each time chosen such that the number of aircraft in a time window is always the same. The advantage is that "the delay is more spread among all aircraft" (Smeltink et al., 2004).

3. Problem description

This section presents an outline of the overall problem formulation that has been adopted, along with a brief description of the inputs required for the proposed real-time taxi movement planning system. After carefully considering the three aforementioned mathematical modeling and solution methods (MILP, metaheuristics and heuristics), a MILP formulation was selected for implementation in the optimization framework of the surface movement planning system. The selected MILP formulation has been implemented in a rolling horizon framework, in order to decompose the single large problem into a number of smaller planning problems, rendering the approach amenable to real-time surface movement planning. Moreover, by periodically advancing the time window, the total airport taxiing schedule can be dynamically updated, allowing to deal with unexpected events or perturbations on the taxiway grid, as well as with flights that enter or leave the taxiway system. It is noted that the trajectories of all surface movements that are planned within a given time window are completely assessed, right up until the end node.

As will be explained in Section 5, the composite objective function adopted in the MILP formulation consists of a weighted combination of the cumulative deviation from the desired CFMU slot times for departures, the taxiing times for both arrivals and departures, and the emissions for all flights. By varying the weighting parameters in the objective function, the emphasis in the optimization can be shifted between the various criteria. The minimum separation standards between the aircraft on the taxiways are assumed to be time-based. A minimum and a maximum taxiing speed have been defined (per aircraft type), between which the optimizer can freely choose any speed, for any flight, on any taxiway segment. One of the novel features in the proposed MILP formulation is that aircraft are also allowed to hold at any node of the taxiway grid. In the proposed model only conflicts between taxiing aircraft are resolved; potential conflicts between taxiing aircraft and aircraft taking off or landing on a runway are left out of consideration. The latter conflicts might occur when taxiing aircraft cross an active runway.

In the proposed formulation, outbound flights are allowed to deviate slightly from their assigned departure slot times, but not to the extent that they infringe the departure slot of the preceding or subsequent flight. This implicitly fixes the aircraft sequences at the departure runways.

The inputs to the MILP-based planning system consist of, (i) a directed graph representing the taxiway grid (node/arc model), (ii) the characteristics and emission parameters for each aircraft (type) considered, (iii) 3–5 potential routes connecting each origin-destination pair (limiting the number of options when routing the aircraft) and, (iv) a fixed flight schedule for inbound and outbound traffic. This flight schedule consists of assigned departure slot times and 'ready-for-pushback times' for outbound flights, landing times for inbound flights, as well as the entry and exit node of each flight.

4. Fuel burn and emission modelling

This section details how fuel burn and gaseous emissions relate to taxiing behavior and how these relationships can be appropriately incorporated into the optimization formulation. The (local) emission substances that have been considered in

this study are, nitrogen oxides (NO_x), carbon monoxide (CO), unburnt hydrocarbons (UHC) and particulate matter (PM). Fuel usage is taken into account as well. There are several pollutants that are directly proportional to fuel burn, including sulphur oxides (SO_x) and carbon dioxide (CO_2), and thus fuel burn can also be viewed as a measure for these pollutants (Visser et al., 2009). Note that only emissions from the aircraft main engines are considered.

To assess the emissions resulting from taxiing operations, it is of paramount importance to first accurately determine the required thrust levels during taxiing operations. Based on the established thrust levels, the fuel usage and associated emissions can then be quantified.

4.1. Thrust levels during taxiing

The timed route of a taxiing aircraft has been modeled using a total of four different types of so-called "actions", viz., (i) Break-away and acceleration, (ii) Taxiing at constant speed, (iii) Idling during a hold, and (iv) Turning. The quantification of the emissions along a route is based on evaluating a sequence of taxiing actions and will be called the "action-based model". For example: when a departing aircraft starts taxiing from the gate, a breakaway action is performed at a relatively high thrust setting which is needed to overcome static friction and to accelerate to taxiing speed. Subsequently, the aircraft taxies at constant speed to the next node. Optionally, the aircraft stops at nodes ("idling during a hold" action), with subsequent break-away actions. Depending on the route structure, "turning actions" might be executed at certain nodes.

Each of the actions causes certain emission and time penalties, all measured relative to taxiing at constant speed. For example, in a break-away action the airplane is accelerated from a standstill to maximum taxiing speed. During this break-away and acceleration action a certain distance is covered. A time penalty is incurred which is defined here as the difference between: (1) the time needed to cover the break-away segment if the aircraft would have taxied at maximum taxiing speed, and (2) the time needed to cover that distance with the aircraft accelerating from standstill to its maximum taxiing speed. Furthermore, since the break-away and acceleration action is executed using increased thrust levels, an associated emission penalty is incurred. The emission penalty for a break-away action (which is always preceded by a holding action or a gate pushback) also includes a correction to allow for the fact that the power has been set to idle thrust instead of taxiing thrust during braking to a standstill on the previous segment (except for the initial break-away from the gate or parking stand).

The mass of a particular pollutant, which is emitted during one of the four taxiing actions, can be modeled using sequential time periods of constant thrust settings, for each aircraft/engine type combination, as expressed by Eq. (1):

$$m_i = \sum_{j=1}^{N_j(i)} n_{engines} \cdot t_{TIM}(j) \cdot FF(\%T(j)) \cdot EI(\%T(j)), \tag{1}$$

where m_i is the mass of the considered pollutant which is emitted during taxiing action i,$n_{engines}$ is the number of engines on the considered aircraft type, j is the identifier of a Time-in-Mode (TIM) period (defined here as a period with constant thrust), $N_j(i)$ is the total number of TIM periods in taxiing action i, $t_{TIM}(j)$ is the duration of TIM period j, $FF(\%T(j))$ is the fuel flow per engine which is dependent on thrust setting $\%T$ (expressed as a percentage of full rated thrust) in TIM period j, and EI($\%T(j)$) is the emission index (grams pollutant per kg fuel burnt) of a certain pollutant, also dependent on thrust setting $\%T$ in TIM period j. The mass of a certain pollutant emitted in a complete taxiing trajectory is calculated by aggregating the emissions from all individual taxiing actions in an aircraft's taxiing trajectory.

The above aircraft emission calculations are based on the so-called Landing-and-Takeoff (LTO) as defined by the ICAO Engine Certification (Visser et al., 2009). These calculations rely on the ICAO Engine Emissions Data Bank (EEDB) to provide fuel flow rates (kg/s) and emission indices (g/kg of fuel) for a large number of engine types at four specific engine power settings (modes): 100% (takeoff), 85% (climb out), 30% (approach), and 7% (idle) (ICAO, 2013). For taxiing operations, fuel flows and emission indices for each thrust setting are obtained by linear interpolation or extrapolation using the fuel flows reported in the EEDB at 7% and 30% engine thrust levels (Chen et al., 2015). The EEDB does not contain any information related to PM emissions. To model the emission of PM, the so-called FOA3.0 method (First Order Approximation method 3.0), as presented in Wayson and Fleming (2009), has been employed in this study.

Fig. 1 illustrates typical behavior of emissions versus engine power setting for a turbofan engine (Ruijgrok and Van Paassen, 2007). As can be seen, the emission levels of NOx and soot increase with increasing thrust settings, whilst the emissions of CO and UHC exhibit a decreasing trend. The levels of PM are not shown in Fig. 1, however, its trend is quite similar to that of soot, i.e., the PM flux increases with increasing thrust levels.

Basic physics are used to calculate the required thrust levels for the four taxiing actions. Applying Newton's law to a point-mass modeled vehicle yields the following expression for the aircraft acceleration a (ignoring taxiway slopes):

$$a = \frac{g}{W}(n_{engines} \cdot \%T.T_{\max} - \mu \cdot W), \tag{2}$$

where $T_{\max}$ is the full rated thrust per engine, W is the aircraft weight and μ is the rolling friction coefficient. Note that in Eq. (2), the aerodynamic drag force has also been neglected. A rolling friction coefficient value $\mu = 0.015$ has been assumed in all taxiing actions (except for the turning action), independent of speed (Daughterty, 2003).

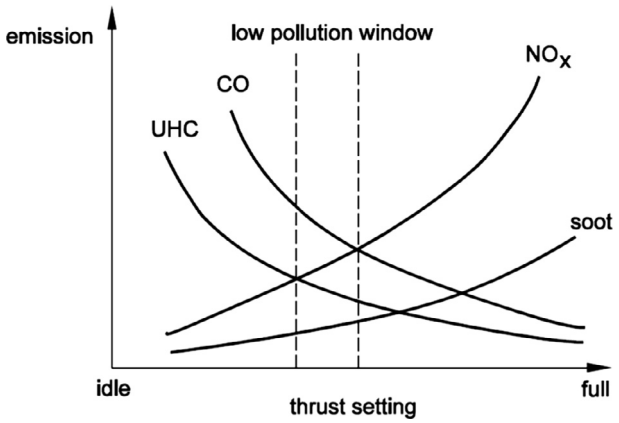

Fig. 1. Emission level versus thrust setting (Ruijgrok and Van Paassen, 2007).

For break-away actions, the acceleration thrust setting $\%T$ and duration t_{TIM} are chosen such that they comply to a desirable acceleration value (around 0.07 g), depending on the aircraft type (Page et al., 2009) and maximum taxiing speed (around 16 kts, depending on the aircraft type). For example, a Boeing 777-300ER with GE90-115B engines at maximum take-off weight (MTOW), requires a 25% thrust setting for the duration of 14 s to achieve a speed of 15.7 kts and an acceleration level of 0.06 g during a break-away and acceleration action. Similarly, in a braking action, the aircraft is decelerated to standstill assuming a fixed deceleration value (around 0.1 g, depending on the aircraft type), with the power set to idle. Although higher deceleration values can be attained, they are not adopted here for reasons of passenger comfort. To more accurately represent high-speed exit behavior, a specific, tailored "braking action" has been defined for this type of operation.

In an action associated to "taxiing at constant speed", the acceleration level a in Eq. (2) is evidently set to zero in order to compute the required thrust setting. Typically, a thrust setting of around 4–5% is found in this type of action.

When aircraft are "idling during a hold", a 3% true idle thrust setting has been assumed in this study. Although an idle thrust level of 4% is indicated in Nikoleris et al. (2011), this value relates to older generations of jet engines. Newer generations of jet engines generally feature a lower ground idle setting and consequently a 3% true ground idle thrust has been assumed herein (Evertse, 2014). An idling during a hold action is always followed by a break-away action.

As indicated in Section 3, the airport surface layout is based on a graph-theoretic representation (Visser and Roling, 2003). The nodes contained in the graph essentially represent intersections of straight taxiway segments. Although turning segments are not explicitly considered in this representation, a "turning action" might be engaged at a particular node based on the identified heading change between the end of a given straight segment and the start of the subsequent straight segment. However, a turning action is engaged only if the angle between the two connecting straight segments exceeds a certain user-specified threshold value. In this study, this threshold angle has been set at 30° by default.

To execute a turning action an increased thrust is required to overcome the additional friction associated to sharp directional changes while taxiing. Thrust levels in turns have been assumed to be at 8% in this study (Evertse, 2014), in conjunction with an aircraft type dependent fixed turning rate (up to 10°/s). To execute a sharp turn an aircraft may have to slow down and to speed up again after completing it. This is reflected in the time penalty that is associated to the turning action. The time penalty associated to a turn is dependent on the value of the angle between two connecting straight segments, and on the characteristics of the aircraft.

4.2. Assumptions in the action-based model

The action-based model has been designed to model aircraft kinematics and emissions, while preserving compatibility with the MILP formulation. This compatibility requirement compromises the fidelity of the model to some extent. In this section, the implications of the associated assumptions and simplifications are presented.

The most significant simplification that has been made in the formulation of the action based model is that speed changes between constant-speed segments are assumed to take place instantaneously. By ignoring the accelerations required to affect such speed changes, the time and fuel penalties associated to such accelerations are ignored as well. To assess the implications of this assumption, the optimal planning results have been analyzed to explore to what extent such speed changes between constant-speed segments actually did occur in the solution. It was observed that most of the time, aircraft are taxiing at or near their maximum speed, so that the influence of this assumption on the optimal taxiing schedules tends to remain small. Indeed, a thorough analysis of the results revealed that accelerations mostly don't need to take place in the optimal solution. In the baseline scenario, for example, it was found that only 25 flights of the 1283 flights feature an accumulated speed change (aggregated along their entire taxi trajectory, excluding accelerations after stops) in excess of 6 m/s; the maximum accumulated speed change observed in any taxi trajectory is 13.4 m/s.

Lastly, during the action of taxiing at constant speed, the emissions are evaluated based on the assumption that the thrust precisely matches the rolling drag. In practice, however, pilots may opt for a somewhat different approach in which they set the throttle slightly higher than the required taxiing thrust for constant speed, while regularly applying the brakes in order to prevent speeding. Although this study did not consider a model for pilots that "ride the brakes", the developed action-based model does permit this particular taxiing technique to be added in future research.

5. Surface movement planning model

In this section, the MILP model for the surface movement planning problem is defined, based on a graph-theoretic representation described in Section 3. Firstly, the decision variables and constraints that are used to define the basic surface movement planning problem (without considering emissions and conflict detection/resolution) will be introduced. Next, the composite objective function will be described, followed by the constraints that define the emission variables. Next, the most important timing, routing and conflict constraints are defined. Finally, the employed iterative optimization (in conjunction with conflict detection and resolution) and time windowing techniques will be described in some detail.

5.1. Basic decision variables

The basic surface movement planning problem is formulated using *binary routing variables* and *continuous timing variables*. The airport taxiway grid is modeled using a directed graph. The decision variables that have selected in the basic problem formulation are similar to those employed in Clare and Richards (2011). Additional variables related to emissions will be introduced at a later stage.

- The binary variable $X(a,n,m,k)$ defines the routing of each aircraft a within the airport taxiway grid. If $X(a,n,m,k) = 1$, flight a will be taxiing from node n to node m in decision stage k. Evidently, the variable $X(a,n,m,k)$ can take on the value one only if the two nodes n and m are directly connected. The staging variable k is a sequence number: a timed route initially starts at the origin node, having $k = 0$. It then enters its first taxiway segment in $k = 1$. After the first segment, it enters the end node of that segment at $k = 2$, etc. Holding at nodes (e.g. to allow other aircraft to pass) is possible by having $n = m$. The MILP problem is formulated such that a hold at a node is made for every *even* value of k (but in most cases a hold will have a duration of zero seconds in the solution).
- The continuous variable $T(a,k)$ is defined as the time that aircraft a enters a node at stage k. In other words, the timing variable $T(a,k)$ attaches a start time to each route decision $X(a,n,m,k)$.

It is noted that the stage variable k runs from zero to the maximum number of route stages, $k_{max}(a)$. The value of k_{max} should be judiciously selected for each taxiing aircraft a. Evidently, the value of k_{max} should at least be equal to the value corresponding to the shortest route from origin to destination in terms of the number of encountered nodes. The value of k_{max} should also not be taken too large, as this increases the number of decision variables and therefore results in a sharp increase in the computational load associated to resolving the planning problem.

Fig. 2 illustrates an example of a simple timed route involving 3 nodes (represented by squares). As indicated earlier, holding at nodes can only take place for even value of the stage variable k (with the exception of the destination node). Note

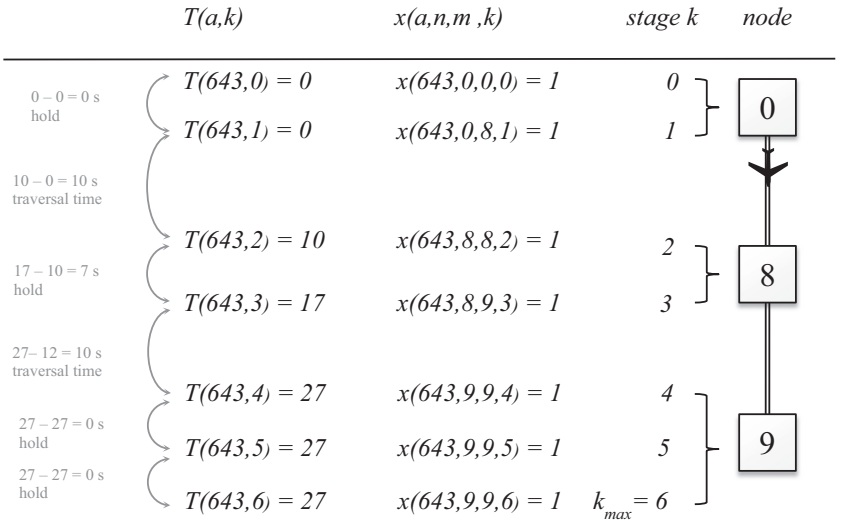

Fig. 2. An example timed route for flight 643, traveling from gate node 0 to destination node 9.

that in this example holding takes place at node 8 at stage $k = 2$. Also note that the flight reaches its destination node 9 at stage $k = 4 < k_{max} = 6$. Zero holding steps are added until the maximum value of the stage k has been reached. This will be discussed in more detail in Section 5.4

Summarizing, the pair $X(a,n,m,k)$ and $T(a,k)$ define that flight a starts taxiing from node n to node m in decision stage k. The flight starts taxiing that segment at $T(a,k)$. From now on, the pair of a $X(a,n,m,k)$ and $T(a,k)$ will be referred to as the "planning step" at stage k. A planning step that results in a segment being traversed will be referred to as a *movement step*. A planning step where no movement occurs (so where $n = m$), will be referred to as a *holding step*.

5.2. Composite objective function

The objective function considered in this study is a weighted combination of, (i) the time offset between the assigned CFMU runway departure time and the time at which the destination node (the runway) is reached, for all departures within the planning horizon, (ii) the taxiing time, for all arrivals and departures within the planning horizon, and (iii) the emissions resulting from all surface movements within the planning horizon. In mathematical form, the composite performance index to be minimized can be expressed as:

$$J = \sum_{a \in A_{dep}} T_{abs}(a) + k_{norm\ taxi} \cdot k_{taxi\ time\ wt} . \sum_{a \in A} T(a, k_{\max}) + \sum_{xx \in XX} \left[k_{norm\ xx} . k_{emission\ wt}(xx) . \sum_{a \in A} \sum_{k=0}^{k_{\max}(a)} (Z_{xx}(a,k) + Y_{xx}(a,k) + W_{xx}(a,k)) \right] \tag{3}$$

The first component in Eq. (3) aims to minimize the absolute value of the arrival time deviation at the specified destination node (typically a runway entry node) measured against the assigned CFMU slot time, aggregated for all flights a of the departure set A_{dep} within the considered planning horizon. More specifically, the absolute time difference $T_{abs}(a)$ is defined here as follows:

$$\forall a \in A_{dep} : T_{abs}(a) = |T(a, k_{\max}) - T_{CFMU}(a)|, \tag{4}$$

where $T_{CFMU}(a)$ is the assigned slot time of flight a at its destination node (i.e., the desired time at which the runway entry node should be reached), and $T(a,k_{max})$ is the actual time of arrival at the destination node. In order to encode the absolute signs into the MILP formulation, Eq. (4) is rewritten as:

$$\begin{aligned} &\forall a \in A_{dep} : T(a, k_{\max}) - T_{abs}(a) \leqslant T_{CFMU} \\ &\forall a \in A_{dep} : -T(a, k_{\max}) - T_{abs}(a) \leqslant -T_{CFMU}(a) \end{aligned} \tag{5}$$

It is noted that the first component of the objective function (3) is not multiplied by a weighting factor and is therefore always considered in the optimization process. The reason to always include this first component is to ensure that the timeslot deviations remain small in all cases, so that the pre-assigned aircraft departure sequence at the runway can be maintained in the optimal planning solution. However, since the inclusion of the first component in the objective function is not sufficient to provide a guarantee for a correct departure sequence at the runway, an additional measure is implemented in the form of a hard constraint that limits the permissible CFMU slot time deviation to a small specified range for each departing aircraft. Note that as a result of these constraints, there is a clear upper bound on the value that the cumulative departure slot time deviation can take.

The second component of Eq. (3) considers the weighted total taxiing time for the arrivals and departures within the planning horizon. The value of the metric "total taxiing time" is normalized by a factor $k_{norm\ taxi}$, so as to ensure that the total cumulative taxiing time is more or less equitably represented relative to cumulative slot time deviation in the composite objective function. The parameter $k_{taxi\ time\ wt}$ in Eq. (3) is a user-customizable weight factor (typically set to zero, one, or a very large positive value, depending on the specific case considered).

The third component in the composite objective function (3) considers the emissions and fuel consumption. For each pollutant xx of the set of emission products XX, the emitted masses resulting from the holding/constant speed taxiing actions $Z_{xx}(a,k)$, the break-away and braking actions $Y_{xx}(a,k)$ and the turning actions $W_{xx}(a,k)$ are aggregated for all surface operations within the planning horizon. The values of emission substances xx are normalized by a factor $k_{norm\ xx}$ in order to ensure that all constituents are equitably represented in the objective function. More specifically, the normalization factor for each product xx is determined as the ratio of maximum permissible CFMU slot time deviation per flight and the average emitted mass of product xx per flight. The average mass of an emitted product has been calculated by dividing the total airport emissions of that particular product by the total number of flights, assessed in an optimization scenario where only the first component of the composite performance index (3) is considered and all conflict constraints are de-activated. This way, if an aircraft emits the average pollutant mass along its optimal trajectory, its contribution to the objective function will be equal to the maximum permissible CFMU slot time deviation (i.e. the maximum value per flight of the first component in the objective function (3)).

Setting the user-customizable weight factor $k_{emission\ wt}$ in Eq. (3) allows the prioritize the minimization of any emission product xx to a desired level. It is noted that the set XX includes "fuel-consumed" (serving as a proxy for CO_2 emissions). The values of the normalization factors employed in the case study are listed in Table 1.

5.3. Emission variables

To enable the assessment of the emission objective, three different emission variables have been defined for each emission product *xx*. Each of the three defined emission variables will be discussed separately in the following subsections.

5.3.1. Idling and constant speed emissions, $Z_{xx}(a,k)$

The variable $Z_{xx}(a,k)$ defines both holding emissions at even values of the planning stage k (those are always holding steps, although possibly of zero duration) and constant-speed-taxiing emissions at odd values of k (those are always movement steps, except at the destination node). An emission associated to a movement step is defined within the linear constraint set as follows:

$$\forall a, k_{odd} : Z_{xx}(a,k) = \dot{m}_{xx\ taxiing}(T(a,k+1) - T(a,k)), \tag{6}$$

where $\dot{m}_{xx\ taxiing}$ is the mass flow for emission *xx* during taxiing at constant speed and k_{odd} relates to the odd values of planning stage k. Note that the term $(T(a,k+1) - T(a,k))$ in Eq. (6) is the time it takes to traverse the taxiing segment. In a similar fashion, the idling emission cost in a holding step is defined as:

$$\forall a, k_{even} : Z_{xx}(a,k) = \dot{m}_{xx\ idling}(T(a,k+1) - T(a,k)), \tag{7}$$

where $\dot{m}_{xx\ idling}$ is the idle emission mass flow of product *xx* and k_{even} relates to the even values of planning stage k. In Eq. (7), the term $(T(a,k+1) - T(a,k))$ represents the time the aircraft was holding at the node.

5.3.2. Break-away and acceleration emissions, $Y_{xx}(a,k)$

The acceleration emission variable, $Y_{xx}(a,k)$, depends on the holding time that preceded the segment. If the holding time was zero, the acceleration emission will be zero as well.

The following indicator constraints (Clare and Richards, 2011), define the acceleration step emission costs that were used in the objective function:

$$\forall\ a, k_{odd} : D_{acc}(a,k) = 0 \rightarrow Y_{xx}(a,k) = \frac{m_{xx\ break-away}}{t_{threshold}}(T(a,k) - T(a,k-1)) \tag{8}$$

$$\forall\ a, k_{odd} : D_{acc}(a,k) = 1 \rightarrow Y_{xx}(a,k) = m_{xx\ break-away}, \tag{9}$$

where D_{acc} is a binary operator that indicates whether there is a "partial hold" ($D_{acc} = 0$) or a "full hold" ($D_{acc} = 1$) where the aircraft comes to a complete stop. A partial holds concerns a hold shorter than $t_{threshold}$ (assumed to be 5 s in this study). The time interval $(T(a,k) - T(a,k-1))$ in Eq. (8) represents the holding time at the node and $m_{xx\ break\text{-}away}$ is the emission mass when performing a break-away and acceleration action. In case of a partial hold, the acceleration action is only penalized proportionally to the holding time. The binary variable D_{acc} is enforced as follows:

$$\forall\ a, k_{even} : T(a,k+1) - T(a,k) - M \cdot D_{acc}(a,k+1) \leqslant t_{threshold} \tag{10}$$

$$\forall\ a, k_{even} : T(a,k+1) - T(a,k) - M \cdot D_{acc}(a,k+1) \geqslant t_{threshold} - M \tag{11}$$

These are big-M constraints that force D_{acc} to zero if the flight performs a partial hold (a hold shorter than $t_{threshold}$ and thus no full stop), and to one if the flight waits longer than $t_{threshold}$ at the node (a full stop). Since holding steps only take place at even values of k, these constraints are not enforced for odd values of k.

5.3.3. Turning emissions, $W_{xx}(a,k)$

The emissions as a result of taxiing sharp turns, $W_{xx}(a,k)$, will only be activated if the track angle between two subsequent (connected) segments exceeds the aircraft-dependent threshold angle. The turning emission cost is defined as follows:

$$\forall\ a, k_{odd}, \{(n_1,m_1)\} : X(a,n_1,m_1,k) = 1 \rightarrow W_{xx}(a,k+2) = \sum_{n_2,m_2}(X(a,n_2,m_2,k+2) \cdot \dot{m}_{xx\ turning} \cdot tpf(a) \cdot \alpha(n_1,m_1,n_2,m_2) + m_{xx\ partial\ hold}) \tag{12}$$

The node variables (n_1,m_1) and (n_2,m_2) in Eq.(12) describe the turn's primary (entry) and secondary (exit) segment, respectively (see Fig. 3), $\dot{m}_{xx\ turning}$ is the emission mass flow during turning, $tpf(a)$ is the aircraft's turning penalty factor (reciprocal of turning speed in seconds per degree), $\alpha(n_1,m_1,n_2,m_2)$ is the intersection angle between the primary segment (n_1,m_1) and connected secondary segment (n_2,m_2), and $m_{xx\ partial\ hold}$ is the emitted pollutant *xx* for the partial break-away after the turn. After traversing any segment at stage k, a holding step is always inserted at the subsequent stage $k+1$ (mostly with a duration of zero seconds in the solution), before traversing the next segment at stage $k+2$; this explains the $k+2$ index in the emission variable W_{xx} in Eq. (12).

Table 1
The normalization factors employed in the case study.

Criterion	Normalization factor
Fuel-consumed (kg)	0.11394
PM emitted (g)	1.91779
UHC emitted (g)	0.03153
NOx emitted (g)	0.02455
CO emitted (g)	0.00234
Taxiing time (s)	0.02312

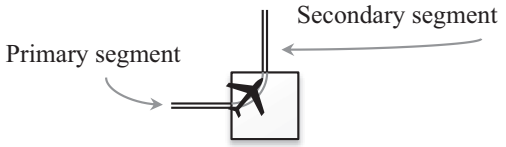

Fig. 3. The primary and secondary segments connecting a turn; the square represents a node.

5.4. MILP constraints

5.4.1. Boundary conditions

The desired initial location of a flight is enforced by the following constraint:

$$\forall\ a : X(a, n_0(a), n_0(a), 0) = 1, \tag{13}$$

where $n_0(a)$ is the specified origin node of each flight a. For departures, the initial time is enforced as follows:

$$\forall\ a \in A_{dep} : T(a, 0) \geqslant T_{pushback\ ready}(a), \tag{14}$$

where $T_{pushback\ ready}(a)$ is the specified pushback ready time of departure a. Eq. (14) ensures that the actual start time must be equal or later than the time that flight a is ready to enter the taxiway grid. Arrivals have to leave the initial node immediately after vacating the runway (i.e. no hold at entry node), giving rise to the following two constraints:

$$\forall\ a \in A_{arr} : T(a, 0) = T_{runway\ exit}(a) \tag{15}$$

$$\forall\ a \in A_{arr} : T(a, 1) = T_{runway\ exit}(a) \tag{16}$$

where $T_{runway\ exit}(a)$ is the specified runway exit time of arrival a.

The desired (final) destination node is encoded as follows:

$$\forall a : X(a, n_f(a), n_f(a), k_{\max}) = 1, \tag{17}$$

where $n_f(a)$ is the specified destination node of each flight a. It is noted that the arrival time of a flight at a destination node is not enforced as a boundary condition in this formulation. Instead, these conditions are governed by the first two components of the objective function (3), as explained in Section 5.2.

5.4.2. Routing constraints

An important routing constraint concerns the *planning activity* constraint that ensures that each flight a has precisely one positive route decision for each planning stage k:

$$\forall\ a, k : \sum_{n=0}^{n=N_n} \sum_{m=0}^{m=N_n} X(a, n, m, k) = 1, \tag{18}$$

where N_n represent the maximum node ID in the airport graph.

Another important constraint included in the formulation concerns the *route continuity* constraint. This constraint enforces that when a flight has moved to a certain node at stage k, the flight must move from that node in the next planning stage $(k + 1)$. It is recalled that in the proposed formulation the routing variables in the planning solution constantly alternate between a moving step $(n \neq m)$ for every odd value of k and a holding step $(n = m)$ for every *even* value of k. Going from a moving step to a holding step is constrained as follows:

$$\forall\ a, k_{odd}, m; n \neq m : \sum_{n=0}^{n=N_n} X(a, n, m, k) = X(a, m, m, k + 1) \tag{19}$$

Similarly, going from a holding step to a moving step the following constraint applies:

$$\forall\ a, k_{even}, n; n \neq p; n \neq n_f(a) : X(a,n,n,k) = \sum_{p=0}^{p=N_n} X(a,n,p,k+1), \tag{20}$$

where p is any node of the taxiway grid that is directly connected to node n and which has not been visited before. The destination node is not included in the above constraint formulation, because if the destination node $n_f(a)$ has already been reached at a stage $k < k_{max}$, the following constraint applies:

$$\forall a, k : \sum_{n=0}^{n=N_n} X(a,n,n_f,k) = X(a,n_f,n_f,k+1) \tag{21}$$

This constraint enforces that when the holding step has been reached at the destination node, the next step is a holding step at the destination node as well.

5.4.3. Timing constraints

Timing constraints couple the routing variables to the timing variables, so that timed routes are being formed. The following constraint ensures compatibility with the maximum taxi speed limit:

$$\forall\ a, k : T(a,k) + \sum_{n=0}^{n=N_n} \sum_{m=0}^{m=N_n} \left(\frac{L(n,m)}{V_{\max}(a)} X(a,n,m,k) \right) \leqslant T_{penalty}(a,k) + T(a,k+1), \tag{22}$$

where the parameter $L(n,m)$ is the length of segment (n,m) and $V_{max}(a)$ is the maximum speed of flight a. The variable $T_{penalty}(a,k)$ is the sum of all time penalties on the segment, (possibly) comprising a turning time penalty, and an acceleration time penalty:

$$T_{penalty}(a,k) = T_{turn\ penalty}(a,k) + T_{acc\ penalty}(a,k) \tag{23}$$

The time penalties $T_{turn\ penalty}(a,k)$ and $T_{acc\ penalty}(a,k)$ in Eq. (23) associated to, respectively, turn and breakaway and acceleration actions on a segment, are evaluated in a fashion similar to the corresponding emission penalties (see Section 5.3). More specifically, the turn time penalty is encoded as:

$$\forall\ a, k_{odd}, \{(n_1,m_1)\} : X(a,n_1,m_1,k) = 1 \rightarrow T_{turn\ penalty}(a,k+2) = \sum_{n_2,m_2} (X(a,n_2,m_2,k+2) \cdot tpf(a) \cdot \alpha(n_1,m_1,n_2,m_2)) \tag{24}$$

The parameters in Eq. (25) are described in Section 5.3.3.

Similarly, the time penalty associated to a (partial) break-away and acceleration action is encoded as:

$$\forall\ a, k_{odd} : D_{acc}(a,k) = 0 \rightarrow T_{acc\ penalty}(a,k) = \frac{t_{full-hold}}{t_{threshold}} (T(a,k) - T(a,k-1)) \tag{25}$$

$$\forall\ a, k_{odd} : D_{acc}(a,k) = 1 \rightarrow T_{acc\ penalty}(a,k) = t_{full-hold}, \tag{26}$$

where D_{acc} is the binary operator defined previously in Section 5.3.2. The parameter $t_{full\text{-}hold}$ concerns the time lag of an aircraft that starts to accelerate from standstill to the final speed, relative to an aircraft that travels the same distance at constant (final) speed. It is noted that the distance required for acceleration is usually much smaller than the length of a taxiway segment.

The minimum traversing speed is enforced with the following constraint:

$$\forall\ a, k_{odd} : T(a,k) + \sum_{n=0}^{n=N_n} \sum_{m=0}^{m=N_n} \left(\frac{L(n,m)}{V_{\min}(a)} X(a,n,m,k) \right) \geqslant T_{penalty}(a,k) + T(a,k+1) \tag{27}$$

The above equation is very similar to the maximum speed constraint given in Eq. (22). However, it only holds for odd values of k, since there is no maximum traversal time for holding steps. Consequently, for holding steps, the minimum speed constraint must be omitted.

5.4.4. Conflict constraints

Conflict constraints are introduced to ensure that aircraft conflicts are prevented. As the number of potential separation conflicts on the taxiway grid scales quadratically with the number of surface movements, the number of separation constraints that needs to be included in the MILP formulation to prevent these potential conflicts might be huge in a realistic airport scenario, having a detrimental effect on the computational burden. However, when conflict constraints are ignored in the MILP formulation, the actual number of conflicts observed in the resulting solution turns out to be rather small, even in relatively complex and dense traffic situations. This observation points in the direction of applying iterative optimization to solve aircraft separation conflicts in a computationally efficient manner (Clare and Richards, 2011). In this approach, initially the MILP problem is formulated and resolved without considering the separation constraints. An external program is then

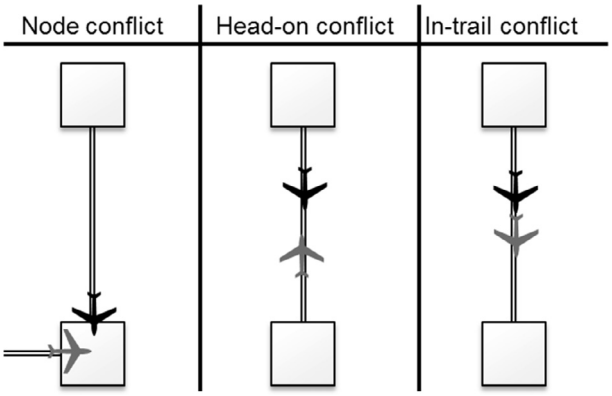

Fig. 4. The three different types of conflicts in a top-view.

evoked that checks the solution for separation conflicts, adds locally separation constraints when necessary, and initiates a new iteration in the optimization process (with the new separation constraints). This process continues until no more conflicts remain.

As illustrated in Fig. 4, three different types of separation conflicts need to be considered, viz. node conflicts, head-on conflicts and in-trail conflict. For the sake of brevity, only the node conflict constraints are described herein. For more details regarding head-on and in-trail conflicts, the reader is referred to Evertse (2014).

A node conflict occurs when two or more aircraft occupy a certain node at more or less the same time, creating a loss of separation (LOS). To prevent such a conflict, a time-based separation is required between aircraft at each node. The minimum required time separation between aircraft at a node is denoted here as t_{sep}.

A node separation constraint sets a minimum time separation of the two concerned aircraft at the considered node. A binary variable D_N is introduced to only activate the conflict constraint if the two specified aircraft actually intend to traverse the node at the specified planning stages. The variable D_N is defined as follows:

$$D_N(a_2, a_2, n, k_1, k_2) = \left(\sum_{m=0}^{m=N_n} X(a_1, n, m, k_1)\right) \cdot \left(\sum_{m=0}^{m=N_n} X(a_2, n, m, k_2)\right), \tag{28}$$

where a_1 and a_2 are the two conflicting aircraft. The binary variable $D_N(a_1, a_2, n, k_1, k_2) = 1$ only if aircraft a_1 and a_2 actually visit node n at stage k_1 and k_2, respectively. To facilitate the MILP implementation, the binary products defined in Eq. (28) are converted into equivalent linear inequalities following the approach of Bemporad and Morari (1999). Using the redefined $D_N(a_1, a_2, n, k_1, k_2)$, the required time separation can be enforced:

$$D_N(a_1, a_2, n, k_1, k_2) = 1 \rightarrow T(a_1, k_1) + M \cdot B_N(a_1, a_2, n, k_1, k_2) \geqslant T(a_2, k_2) + t_{sep} \tag{29}$$

$$D_N(a_1, a_2, n, k_1, k_2) = 1 \rightarrow T(a_1, k_1) + M \cdot B_N(a_1, a_2, n, k_1, k_2) \leqslant T(a_2, k_2) - t_{sep} + M, \tag{30}$$

where $B_N(a_1, a_2, n, k_1, k_2)$ is an binary variable that is introduced to serve as a sequencing switch. The binary switch $B_N(a_1, a_2, n, k_1, k_2) = 1$ only if aircraft a_1 precedes aircraft a_2. Note that the node conflict constraint (30) is relaxed when $B_N = 0$ and thus aircraft a_2 precedes, whilst constraint (29) is relaxed when $B_N = 1$ and thus aircraft a_1 precedes.

It is noted that the minimum speed constraint that is enforced for each surface movement does not represent a physical requirement, but rather it is used here to help ensure a safe (lateral or in-trail) separation distance between aircraft at any given node, to protect against the effects of jet blast. Given the minimum required time separation between aircraft t_{sep}, the distance travelled by an aircraft a leaving a certain node is at least $V_{\min}(a) \cdot t_{sep}$ before that node is reached by another aircraft. Assuming a specified minimum safe separation distance d_{sep} between two aircraft, the requirement for the minimum speed limit automatically follows: $V_{\min}(a) \cdot t_{sep} \geq d_{sep}$.

5.5. Time windowing

The time window feature that has been implemented breaks up the total airport's flight schedule into smaller sequential timeframes, each covering only a fraction of all the flights to be optimized. The following flights are included in a time window calculation:

- Flights that are ready to enter the taxiway system within the considered time window.
- Flights that were already taxiing on the airport at the start of the considered time window, but still need to reach their destination node (these trajectories require the insertion of "virtual" nodes, as will be described later).
- Flights that were already ready for pushback in a previous time window, but did not enter the taxiway system yet.

For flights that are located in between two nodes at the start of a new time window, virtual nodes are created on-the-fly, as in Clare and Richards (2011). A virtual node is a dynamically created node, precisely at the location where an aircraft would be at the start of the new time window. However, when moving across time windows, the creation of virtual nodes sometimes induces rounding errors that make it impossible to exactly meet the timing constraints in the new time window. To resolve this problem, auxiliary time buffers were added in the timing constraints that allow the rounding errors to be absorbed. The time buffers are strongly penalized in the objective function, so that they are negligibly small while feasibility remains guaranteed.

6. Results

This section presents the results of a case study in which the capabilities of the developed real-time taxi movement planning system have been assessed. First, a brief outline of the scenario employed in the case study will be presented. Next, a baseline case is defined and some key results (emissions and taxiing times for arrivals) will be presented relative to the baseline case solution, for a range of different settings of the weighting factors in the objective function. Finally, some computational aspects are discussed.

6.1. Scenario for the case study

The capabilities of the real-time taxi movement planning system have been explored in a test case pertaining to Amsterdam Airport Schiphol in the Netherlands. Schiphol is a major international hub airport, featuring six runways. In this study a directed graph representation of Schiphol airport has been conceived that comprises 131 nodes. The employed scenario features an existing (daily) flight schedule that comprises 1283 inbound and outbound flight movements. During (departure or arrival) peak hours, the scheduled number of flight movements per hour may (slightly) exceed one hundred, whilst during the night time the number of movements remains quite low. Fig. 5 presents an example snapshot of the traffic situation on the taxiway grid, taken during a typical peak hour.

Note that the red[1] lines in Fig. 5 represent uni-directional taxi segments.

The selection of the most appropriate time window settings in the considered scenario has been largely made based on experimental results. The choice essentially represents a compromise between performance and computational demands. Ultimately, a time window size of 60 s and a window advance time of 15 s were selected. Although a time window of just 60 s may seem rather small, it is important to realize that the timed routes of the departure flights are already optimized as soon as they are ready to taxi out. Most departures are ready for pushback some 5–10 min in advance of their optimal taxi-out time, so that the departures are considered in the optimization well in advance.

On the taxiway system, a safe separation distance (jet blast) between two aircraft of 46 m (150 ft) has been assumed in this case study. This particular requirement was extracted from the Australian Civil Aviation Order 20.9, section 5.1.4 (Civil Aviation Safety Authority, 2011). A standard required minimum time separation of 30 s was uniformly applied in this study, which proved to be ample in all conditions (minimum taxiing speed of 2 m/s). The maximum deviation from the CFMU slot time for departures in the numerical experiments was fixed at just 10 s (late or early). This way, the aircraft departure sequence at the runway entry is implicitly fixed, which is desirable for airports in order to maintain maximum runway throughput capacity.

6.2. Results for the baseline case

The results obtained for the various emission criteria will be presented relative to the results obtained in a defined baseline case. This baseline case relates to an optimization run in which the weight factors pertaining to fuel-consumed and unburnt hydrocarbons (UHC) are both set to one, while the remaining weight factors in the objective function are set to zero. The results obtained in the baseline case are presented in terms of the outcomes for the various key performance indicators (emissions, departure slot time offsets, and taxiing times for arrivals and departures), aggregated over all surface movements. The cumulative arrival taxiing time and emission outputs obtained in the baseline scenario are listed in Table 2. Note that the results with respect to the taxiing times for departures and the departure slot time offsets have not been included in Table 2; the absolute value of the slot time deviation for each departing flight proved to remain within a one second time span in the baseline solution.

The rightmost column of Table 2 shows how much additional emissions are produced in order to resolve the separation conflicts that occur in the baseline case. These results are obtained by comparing the results of the baseline case with the results obtained in a scenario where all aircraft would taxi according to their own "ideal" taxi plan (unimpeded solution). An ideal taxi plan is the preferred taxi plan for each individual surface movement in the absence of any other traffic. Despite the dense traffic schedule and the many potential conflicts this brings about, the results in Table 2 clearly show that the increase in emissions relative to the unimpeded solution is just a few percent for any emission product.

[1] For interpretation of color in Fig. 5, the reader is referred to the web version of this article.

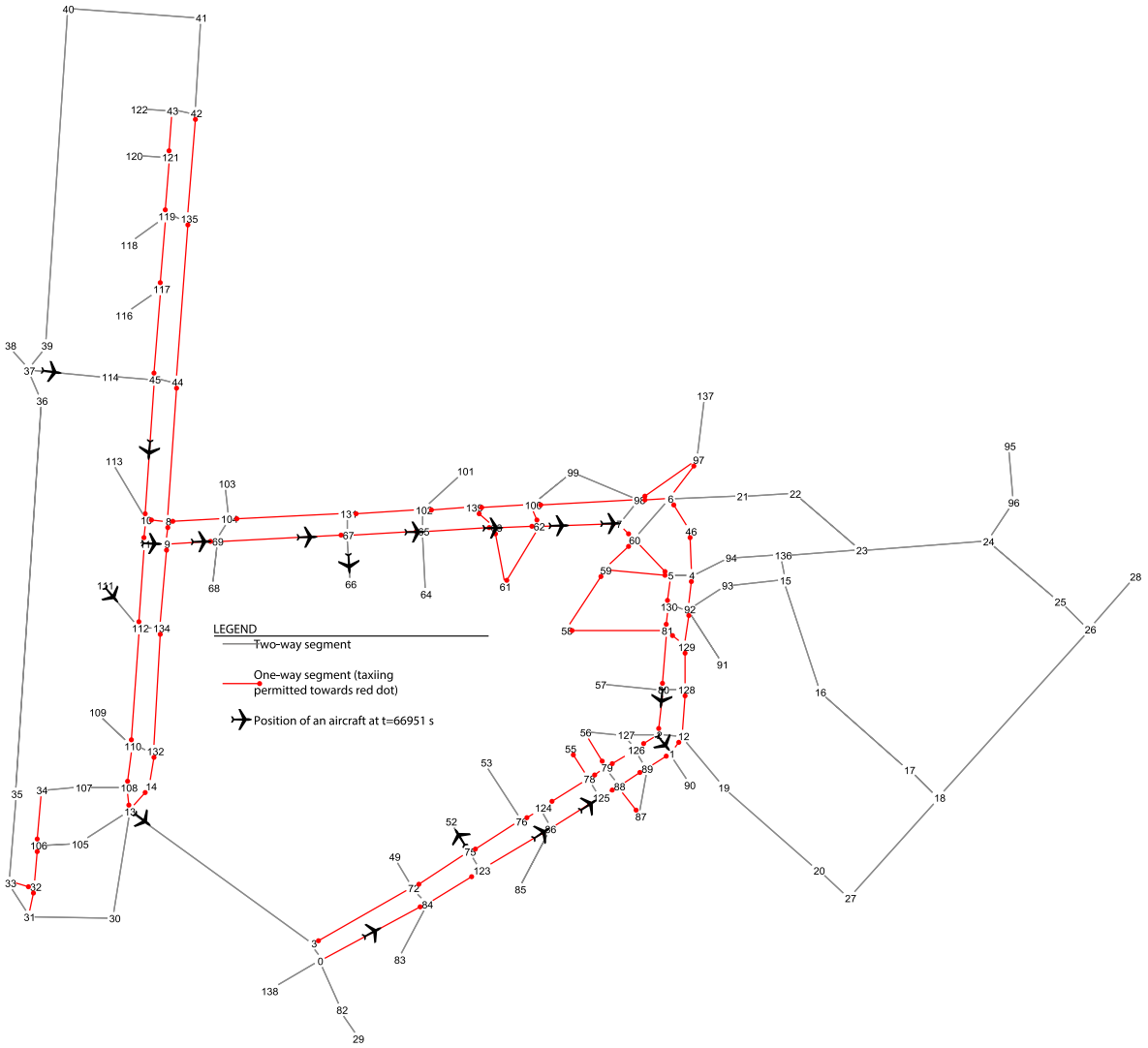

Fig. 5. An example snapshot of the situation on the taxiway grid during peak hours, in the baseline case.

Table 2
The key performance indicators for the baseline scenario.

Performance indicator	Value	Deviation from unimpeded solution
Fuel-consumed (kg)	114,738	+1.9%
PM emitted (g)	6811	+1.8%
UHC emitted (g)	413,583	+1.7%
NOx emitted (g)	531,311	+1.7%
CO emitted (g)	5,604,661	+2.1%
Taxiing time arrivals (s)	281,991	+2.4%

It is noted that during peak hours, the baseline solution occasionally features surface movements that do not take the shortest route from origin to destination node, but rather take a detour in order to avoid conflicts or to meet the CFMU slot times.

6.3. Results for various emission criteria

Optimal surface movement planning solutions have been generated for a range of settings of the emission weighting factors in the composite objective function. Fig. 6 shows the results that are obtained when all weighting factors in the objective

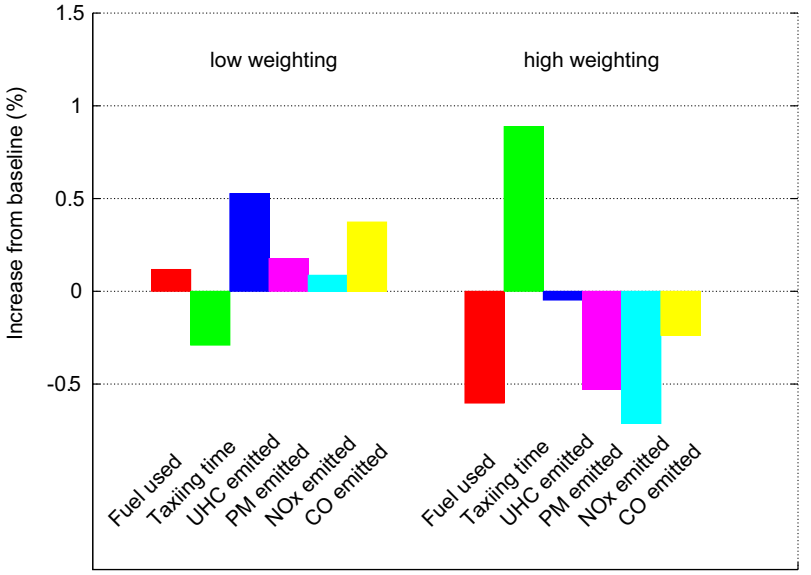

Fig. 6. Key Performance Indicator values obtained in the fuel-optimized solution.

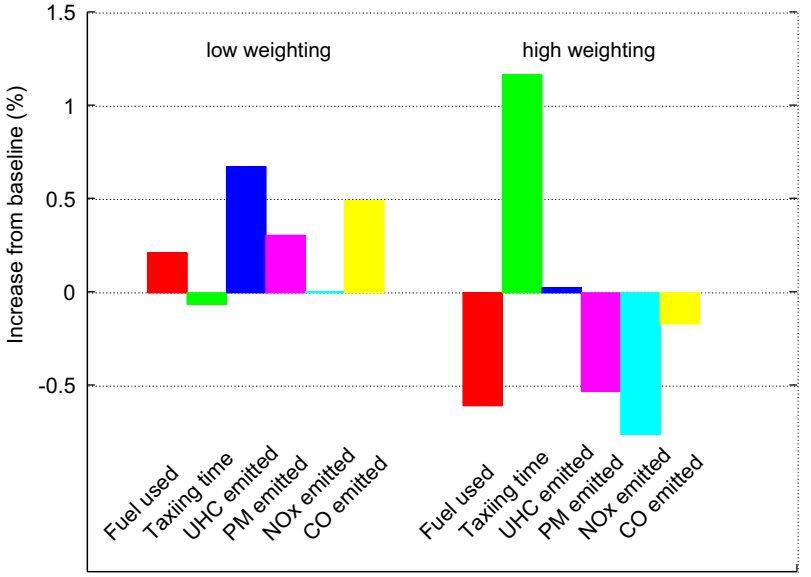

Fig. 7. Key Performance Indicator values obtained in the NO_x-optimized solution.

are set to zero, except for fuel-consumed. More specifically, fuel-optimized results are shown for two distinctly different values of the weight factor for fuel-consumed, viz., a low weighting (i.e., weight factor 1), and a high weighting (i.e., weight factor 200). A close inspection of the results presented in Fig. 6 reveals that, while all emission products (including fuel-consumed) slightly increase for a low weighting on fuel-consumed, they all decrease in the case of a high weighting of fuel-consumed in the objective function. The decrease of the emissions in the latter case clearly comes at the expense of the cumulative taxiing time for arrivals. Furthermore, it is noticed that all relative increases/decreases remain rather small.

In Fig. 7 the results are shown pertaining to the case where the primary criterion is the mass of emitted NO_x. In this case, all weight factors in the composite objective function are again set to zero, with the exception of NO_x (again, a low and a high weighting is specified). A comparison of the NO_x-optimized results presented in Fig. 7, with the fuel-optimized results in Fig. 6 shows that the two solutions are actually quite similar.

The results obtained when optimizing for CO emissions, shown in Fig. 8, exhibit a somewhat different behavior with respect to the arrival taxiing time metric. Indeed, the solution that is obtained when a high weight factor to CO is applied,

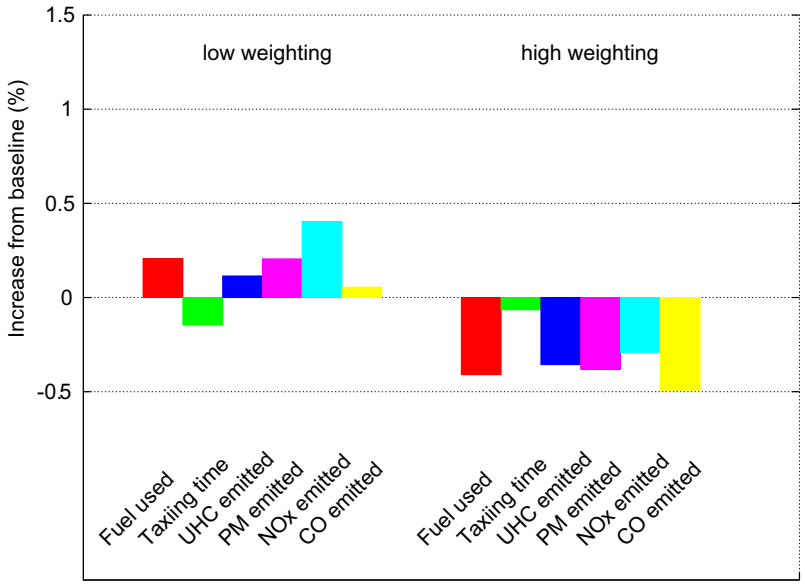

Fig. 8. Key Performance Indicator values obtained in the CO-optimized solution.

permits a reduction in CO emissions of 0.5%, while still reducing the arrival taxiing time. This particular behavior results from the fact that arriving aircraft typically produce more CO (and UHC) than departures while taxiing. Since arriving aircraft have a lower gross weight than departing aircraft, the thrust setting of arriving aircraft during taxiing is typically lower and therefore the emissions of CO and UHC of arriving aircraft are higher. Thus, when the optimization process is focused on minimizing the emissions of CO (and UHC), the arrivals flights are implicitly prioritized over the departing flights.

It is noted that optimization with respect to UHC provides similar results to the CO optimization case. Optimization with respect to CO (or UHC) appears to offer an attractive compromise solution: while the emissions of CO and UHC are minimal in this solution, the emissions of NO_x and PM are very near to the minimum levels that can be attained, while the cumulative taxiing times for arrivals are also kept in check.

The final case presented, relates to optimization with the focus on PM emissions. The results that are obtained when all weighting factors in the objective function are set to zero, except for PM, are shown in Fig. 9. It can be observed that the behavior of the PM-optimized solution is again quite similar to that of the fuel-optimized solution, resulting in only a marginal improvement in terms of PM emissions.

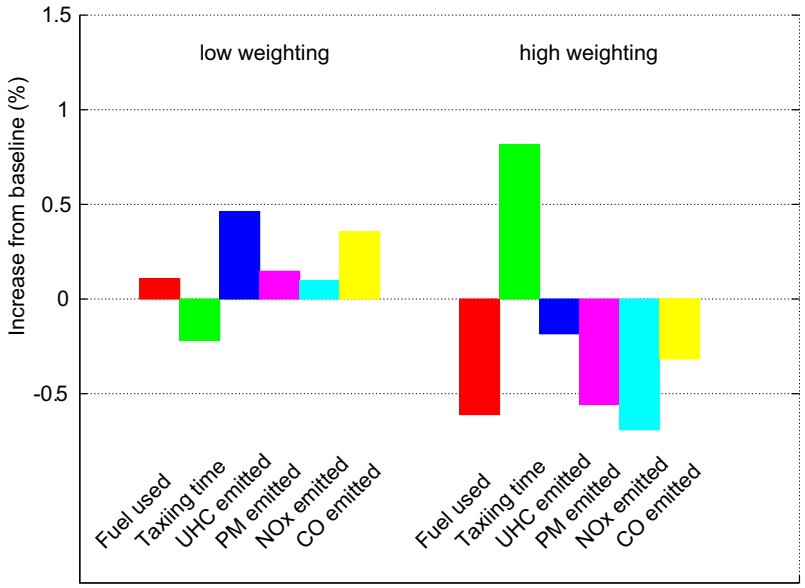

Fig. 9. Key Performance Indicator values obtained in the PM-optimized solution

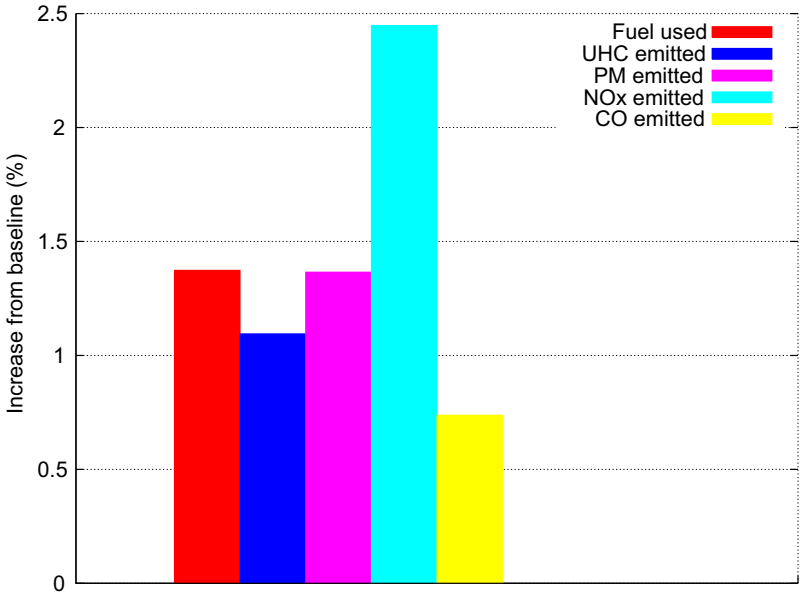

Fig. 10. Environmental Performance Indicator values obtained in the taxiing time optimized solution.

It is noted that in all cases where high emission weighting factors are applied, the resulting slot time deviations for departing flights no longer remain negligible. While the cumulative deviation from the CFMU slot times was as low as 10 s for cases with low emission weight factors, it was as high as 2000 s for some cases with high emissions weight factors. By emphasizing the emission component in the objective function, the influence of the slot time deviation component in the objective function is attenuated in the optimization process. Although the majority of the departing flights still exhibit an offset of the assigned slot time that is less than one second in absolute value, there is also a significant number of departing flights that now sustain the maximum permissible deviation from the CFMU slot time (10 s).

6.4. Results for the taxiing time criterion

Optimization experiments have also been carried out for a case in which the emission criteria were omitted from the objective function, and instead the total taxiing time for both arrivals and departures is included (using a weight factor $k_{taxi\ time\ wt} = 1$). A close inspection of the results for this case presented in Fig. 10 reveals that all emissions have increased relative to the baseline case by an amount ranging from 0.5% to 2.5%, depending on the specific emission product considered. Evidently, relative to the emission-optimization cases where a high weighting is applied to emission products in the objective function (presented in the previous Subsection), the emission output is even increased further, to a range of in between 1% and 3%, depending on the product. This clearly shows the relevance of including emission considerations in the optimization of the surface movement planning. It is noted that most of the increase in cumulative emissions in the taxiing time optimized solution, relative to the emission-optimized cases, is due to an increase in hold time at the nodes.

6.5. Computational aspects

In order for the surface movement planning system to be able to operate in real-time, it is important that it does not take more time than the (15 s) re-planning interval to resolve the MILP problem in each time window. All optimization runs were performed on a notebook with mid-range hardware as of late 2013, i.e., a 2.4 GHz Intel Core i5 4258U processor, with 8 GB DDR3L SDRAM running at 1600 MHz. CPLEX version 12.5 was used for resolving the MILP problem in each time window.

All the optimization experiments featured quite similar computational times, regardless of the weighting factors that were employed in the composite performance index. The time needed to resolve the MILP problem for each time window heavily depends primarily on the number of binary routing variables defined within the time window, in conjunction with the number of separation conflicts that need to be resolved. While for the vast majority of time windows the MILP problem could be readily resolved within the allowed time, for a few time windows the complexity of the problem was such that the required computational time (vastly) exceeded the refresh rate of 15 s. Typically, surges in computational load started to emerge when the number of binary routing variables exceeded about 15,000, in combination with a number of potential separation conflicts in excess of 150. Fortunately, the problem of excessive computational times can be readily resolved by operating the surface movement planning system in so-called "Degraded Mode". In the Degraded Mode (DM), the possibility of aircraft to hold at nodes is disabled. This simplifies the complexity of the associated MILP problem formulation appreciably,

to the extent that the computational demand can now be kept well within the allotted time slot in any circumstance. It is noted that switching to DM has only limited impact on the performance. The reason for this is that even when the surface movement planning is operated in its regular mode, holding at nodes does not often occurs, and if it does occur, it is generally not more than once per flight. Typically, a slight increase in the taxiing time for arrivals and in the departure slot time deviations is observed when operating in DM (typically of the order of 0.5%). At the same time, there is very little difference in emission output, (typically less than 0.1%) when comparing the normal and the DM runs.

In conclusion, the surface movement planning system is definitely capable of keeping up with the assumed refresh rate of 15 s. When it turns out that there are too many routing variables and separation constraints in the problem, switching to degraded mode is necessary to resolve the problem within the allotted time.

7. Conclusions

The objective of this study was to design, develop and test a real-time airport surface movement planning tool, which is capable of creating conflict-free timed taxiing trajectories for aircraft, while minimizing the total emission of pollutants, fuel usage, departure slot time deviations and taxiing times. Although pilots are not capable yet of accurately following a timed taxiing route in the present-day ATM, it is expected that future developments will make this possible (Visser and Roling, 2003).

The presented tool proved to be capable of making an operationally viable planning, within the computational time limits. Since the planning tool takes into account acceleration times after holds and increased taxiing times in turns, it is expected that all aircraft on the taxiways will be able to follow the optimized taxi planning. Accelerations due to speed changes over adjacent constant-speed segments could not be modeled in this MILP formulation, but it was noticed that significant speed changes across segment boundaries almost never occur in the solution.

A parametric study was conducted to explore the characteristics of the surface planning solutions for a wide range of settings of the weight factors in the objective function. With regard to environmental optimization it was found that the planning solutions tend to be very similar, regardless of the emission product specified in the optimization. However, whether emissions are weakly or highly weighted in the objective function, does have a significant impact on solution behavior. All optimization runs with high weights on the emissions result in a lower emission output of up to 1% per product, compared to the runs with a low weighting of emissions. This improvement in environmental performance typically comes at the expense of increased cumulative taxiing times and larger cumulative slot time deviations. However, when the optimization is carried out with respect to the emission product CO (or UHC), the taxiing times for arrival flights are actually improved when a high weighting is applied in the objective function.

A comparison of emission-optimized solutions with taxiing time-optimized solutions has revealed that emission reductions of up to 3% can be achieved. Although these reductions are modest, they do represent environmental and economical (fuel cost savings) benefits. Therefore, a surface movement planning system, capable of minimizing emissions in conjunction with the total taxiing time, can be a valuable asset for airports that have dense surface movement traffic and stringent environmental requirements.

References

Atkin, J.A.D., Burke, E.K., Ravizza, S., 2010. The airport ground movement problem: past and current research and future directions. In: International Conference on Research in Air Transportation, Budapest, Hungary, 1–4 June 2010, pp. 131–138.

Balakrishnan, H., Jung, Y., 2007. A framework for coordinated surface operations planning at Dallas-Fort Worth International Airport. In: Proceedings of the AIAA Guidance, Navigation, and Control Conference, Hilton Head, SC, 20–23 August 2007.

Bemporad, A., Morari, M., 1999. Control of systems integrating logic dynamics and constraints. Automatica 35 (3), 407–427.

Chen, J., Stewart, P., 2011. Planning aircraft taxiing trajectories via a multi-objective immune optimization. Proceedings of the 7th International Conference on Natural Computation (ICNC), Shanghai, 26–28 July 2011, vol. 4, pp. 2235–2240.

Chen, J., Weiszer, M., Stewart, P., 2015. Optimal speed profile generation for airport ground movement with consideration of emissions. In: Proceedings of the IEEE 18th International Conference on Intelligent Transportation Systems, Las Palmas de Gran Canaria, Spain, 15–18 Sept. 2015, pp. 1797–1802.

Chen, J., Weiszer, M., Stewart, P., Shabani, M., 2016. Toward a more realistic, cost-effective, and greener ground movement through active routing — part I: optimal speed profile generation. IEEE Trans. Intell. Transp. Syst. 17 (5), 1196–1209.

Civil Aviation Safety Authority (Australia), 2011. Civil Aviation Order 20.9 Amendment Instrument 2011 (No. 2). <https://www.legislation.gov.au/Details/F2011C00881>.

Clare, G., Richards, A., 2011. Optimization of taxiway routing and runway scheduling. J. Intell. Transport. Syst. 12 (4), 1000–1013.

Daughterty, R., 2003. A Study of the Mechanical Properties of Modern Radial Aircraft Tires. NASA Tech. Rep. TM-2003-212415.

Evertse, C., 2014. A Low Emissions Taxi Movement Planning Tool (MSc thesis). Faculty of Aerospace Engineering, TU Delft.

Garcia, J., Berlanga, A., Molina, J.M., Casar, J.R., 2005. Optimization of airport ground operations integrating genetic and dynamic flow management algorithms. AI Commun. 18 (2), 143–164.

Gotteland, J.-B., Durand, N., Alliot, J.-M., 2003. Handling CFMU slots in busy airports. In: Proceedings of the 5th USA/Europe Air Traffic Management Research and Development Seminar, Budapest, Hungary, 23–27 June 2003.

Herrero, J.G., Berlanga, A., Molina, J.M., Casar, J.R., 2005. Methods for operations planning in airport decision support systems. Appl. Intell. 22 (3), 183–206.

ICAO Committee on Aviation Environmental Protection (CAEP), 2013. Aircraft Engine Emissions Databank (EEDB).

Marín, A., Codina, E., 2008. Network design: taxi planning. Ann. Oper. Res. 157 (1), 135–151.

Nikoleris, T., Gupta, G., Kistler, M., 2011. Detailed estimation of fuel consumption and emissions during aircraft taxi operations at Dallas/Fort Worth International Airport. Transport. Res. Part D: Transp. Environ. 16 (4), 302–308.

Page, J. et al., 2009. Enhanced Modeling of Aircraft Taxiway Noise, volume 1: Scoping. Contractor's Final Report for ACRP Project 11–02 Task 8, June 2009.

Pesic, B., Durand, N., Alliot, J.-M., 2001. Aircraft ground traffic optimisation using a genetic algorithm. In: Proceedings of the Genetic and Evolutionary Computation Conference (GECCO-2001), San Francisco, CA, 7–11 July 2001.

Ravizza, S., Chen, J., Atkin, J.A.D., Burke, E.K., Stewart, P., 2012. The trade-off between taxi time and fuel consumption in airport ground movement. In: Proceedings of the Conference on Advanced Systems for Public Transport (CASPT12), Santiago, Chile, 23–27 July 2012.
Ruijgrok, G.J.J., Van Paassen, D.M., 2007. Elements of Aircraft Pollution. VSSD, Delft, The Netherlands.
Smeltink, J., Soomer, M., de Waal, P., van der Mei, R., 2004. An optimisation model for airport taxi scheduling. In: Proceedings of the INFORMS Annual Meeting, Denver, CO, 24–27 October 2004.
Visser, H.G., Roling, P.C., 2003. Optimal airport surface traffic planning using mixed-integer linear programming. In: Proceedings of the AIAA's 3rd Annual Aviation Technology, Integration, and Operations (ATIO) Technical Forum, Denver, CO, 17–19 November 2003.
Visser, H.G., Hebly, S.J., Wijnen, R.A.A., 2009. Management of the Environmental Impact of Airport Operations. Nova Science Publishers, New York.
Wayson, R.L., Fleming, G.G., 2009. Methodology to estimate particulate matter emissions from certified commercial aircraft engines. J. Air Waste Manag. Assoc. 59, 91–100.
Weiszer, M., Chen, J., Ravizza, S., Atkin, J.A.D., Stewart, P., 2014. A heuristic approach to greener airport ground movement. In: Proceedings of the IEEE Congress on Evolutionary Computation (CEC), Beijing, China, 6–11 July 2014.